Industrial Crops & Products 143 (2020) 111909

Contents lists available at ScienceDirect

Industrial Crops & Products

journal homepage: www.elsevier.com/locate/indcrop

Extraction of aromatic abietane diterpenoids from *Salvia officinalis* leaves by petroleum ether: Data resolution analysis

Arthur A. Salamatin[a,b,*], Alyona S. Khaliullina[c], Ramil Sh. Khaziev[d]

[a] Institute of Geology and Petroleum Technologies, Kazan Federal University, 18 Kremlyovskaya str, Kazan, 420008, Russia
[b] Institute of Mechanics and Engineering, FRC Kazan Scientific Center, Russian Academy of Sciences, 2/31 Lobachevsky str, Kazan, 420111, Russia
[c] Institute of Fundamental Medicine and Biology, Kazan Federal University, 18 Kremlyovskaya str, Kazan, 420008, Russia
[d] Institute of Pharmacy, Kazan State Medical University, 49 Butlerov str., Kazan, 420012, Russia

ARTICLE INFO

Keywords:
Salvia officinalis
Carnosic acid
Total content
Petroleum ether
Percolation
Resolution analysis

ABSTRACT

Salvia officinalis is the source of a vast variety of compounds valuable for pharmaceutical and food industry. The extractability of lipophilic diterpenoids from *S. officinalis*(L.) by petroleum ether is studied using Soxhlet, reflux, and percolation methods. The binding of the solute to the plant matrix is described by the Hill-Langmuir desorption model. The Monte Carlo sampling method is used to constrain the parameters of the extraction model and perform the resolution analysis of the extraction data. The percolation, followed by extraction at reflux, is demonstrated to be the most efficient method of extraction. The freely available content is estimated to be $y_e = 20.0 \pm 2.9$ mg g^{-1}, while the total content in our case is shown to be 50–55 mg g^{-1} or higher. For engineering applications, the estimate of 60–70 mg g^{-1} is suggested as the upper limit.

1. Introduction

Extracts of *Salvia officinalis* leaves are widely used in the pharmaceutical industry. They contain a diversity of active components (Durling et al., 2007; Lu and Yeap Foo, 2002; Miura et al., 2002; Perry et al., 1999), and exhibit numerous biological activities: antibacterial, antioxidant, antifungal etc. (Kolac et al., 2017; Longaray Delamare et al., 2007; Raut and Karuppayil, 2014). Potentially extracts can treat emerging bacteria strains such as Methicillin-resistant *Staphylococcus aureus* (Longaray Delamare et al., 2007), which are responsible for several difficult-to-treat human infections.

Abietane diterpenoids, such as carnosic acid and its major derivative – carnosol, comprise one of the most valuable groups of sage metabolites (Birtić et al., 2015; Munné-Bosch and Alegre, 2001; Okamura et al., 1994; Schwarz and Ternes, 1992; Thorsen and Hildebrandt, 2003). They demonstrate high antioxidant activity (Huang et al., 1996; Miura et al., 2002), being comparable to those of butylated hydroxyanisole (BHA) and butylated hydroxytoluene (BHT), powerful synthetic antioxidants commonly used as food additives (Chang et al., 1977).

While the biological activity of the target compounds of *S. officinalis* has been widely studied (Birtić et al., 2015), the renewed attention to natural diterpenes requires further development of extraction protocols aimed at quantitative control of the raw material optimized in terms of labour, time, and cost. Therefore, a better understanding of the extraction kinetics is one of the challenging priorities. Two major factors that affect the extraction kinetics of target metabolites could be distinguished: the solvent chosen for extraction, and distribution, storage, and binding of the metabolites within the plant matrix. All these factors should be carefully taken into account in interpreting the extraction data.

The abietane diterpenoids of interest are lipophilic compounds. Thus, non-polar solvents, like petroleum ether (PE), are suggested for extraction (Khaliullina et al., 2017; Xie et al., 2016). The PE fraction contains a number of lipophilic compounds, like monoterpenes, sesquiterpenes, triterpenoids, diterpenoids, sterols, lipids etc. (Anastasaki et al., 2017; Ibrahim, 2012; Kintzios, 2000; Kontogianni et al., 2013; Thorsen and Hildebrandt, 2003). However, only the abietane diterpenoids, like carnosic acid and its derivatives, contain the aromatic ring in their chemical structure. For comparison, the structure of major abietane diterpenoids is shown in Fig. 1. Thus UV-spectrophotometry is suggested (Anastasaki et al., 2017; Kontogianni et al., 2013; Thorsen and Hildebrandt, 2003) for the determination of the sum of diterpenes in PE fraction at the analytical wavelength 285 nm.

The low overall content of the target compounds, i.e., of ~40–60 mg g^{-1} (Jassbi et al., 2013), assumes that the extraction is essentially a desorption process (Bucić-Kojić et al., 2013; del Valle and Urrego, 2012; Durling et al., 2007; Liu, 2015; Perrut et al., 1997), and its primary characteristic is the equilibrium desorption isotherm. The

* Corresponding author at: Aerohydromechanics Dept, Kazan Federal University, 18 Kremlyovskaya str, Kazan, 420008, Russia.
E-mail addresses: arthouse131@rambler.ru (A.A. Salamatin), anela_90@mail.ru (A.S. Khaliullina), xaziev@inbox.ru (R.S. Khaziev).

https://doi.org/10.1016/j.indcrop.2019.111909
Received 21 July 2019; Received in revised form 22 September 2019; Accepted 25 October 2019

Nomenclature

A [–]	solution absorbance at the wavelength 285 nm
c [ppm]	current solution concentration during extraction
c_0 [ppm]	concentration scaling factor for the equilibrium desorption isotherm
c^∞ [ppm]	solution concentration in equilibrium with the target compounds y^∞ remained in the raw material
d [mm]	cell thickness, for the absorbance A measurements
$E_{1cm}^{1\%}$ [dL cm^{-1} g^{-1}]	specific absorbance coefficient, i.e. absorbance of carnosic acid per 1 dL of petroleum ether solution in cell
k [–]	Hill coefficient (index)
L [mL g^{-1}]	solvent volume used for extraction per unit dry mass of raw material
m [g]	dry mass of the ground raw material used for extraction
n [–]	dilution factor
t [min]	current time
T [min]	total extraction time
x [%]	percent ratio of target compounds mass extracted from the raw material to the total (dry) mass of the material
y [%]	ratio of target compounds mass, which are still in the raw material to the dry mass of the raw material
y_e [%]	target compound mass content that is easily available for extraction, i.e. stored in chloroplasts
y_h [%]	target compound mass content that is strongly bound to the raw material matrix, i.e. adsorbed on the surface of ER and IM
y_0 [%]	total content of target compounds in the unit dry mass of the raw material
y^∞ [%]	current content of the target compounds in the raw material that is in equilibrium with the solute concentration c^∞ in the solvent
Y_0 [%]	pre-extracted amount of target compounds
ER	endoplasmic reticulum
IM	intracellular membranes
PE	petroleum ether
SI	supplementary information

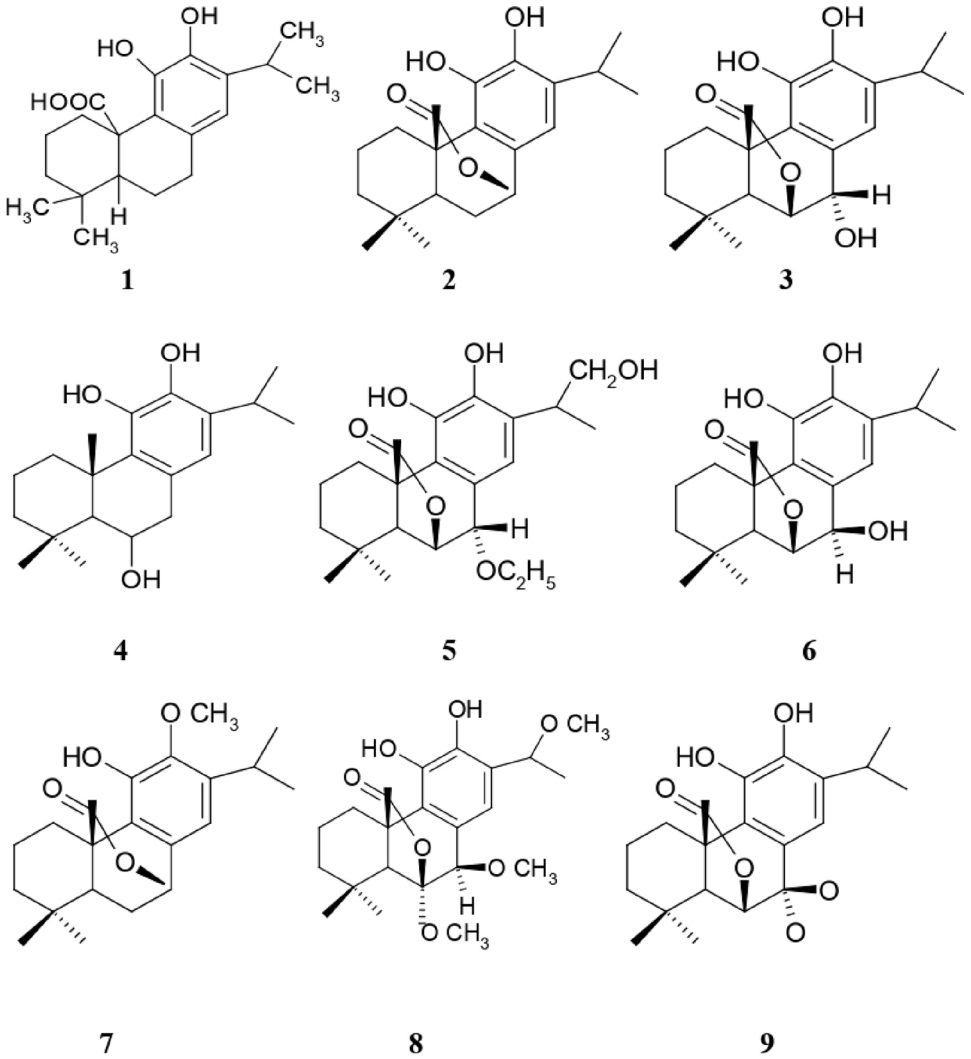

Fig. 1. Structures of carnosic acid (1) and of phenolic diterpenes similar to carnosic acid (1): 1 – carnosic acid; 2 – carnosol; 3 – rosmanol; 4 – isorosmanol; 5 – rosmanol-7-ethyl ether; 6 – epirosmanol; 7 – 12-O-methylcarnosol; 8 – 6,7-O-dimethylepirosmanol; 9 – galdasol.

latter one relates the equilibrium solution concentration, $c = c^{\infty}$, and the corresponding content of target compounds, $y = y^{\infty}$, in the solid phase (plant matrix), predicting the current driving force of extraction in the course of system equilibration.

The choice of the correct, physically meaningful desorption curve depends on the nature of ligand-to-protein binding (Wyman and Gill, 1990). For the rosemary leaves (as the most studied diterpenes-containing herb), existence of at least two storage mechanisms is confirmed (Kleinig, 1989; McGarvey and Croteau, 1995; Munné-Bosch and Alegre, 2001). On one hand, carnosic acid was found in the chloroplasts and Intracellular Membranes (IM) (Knudsen et al., 2018). On the other hand, some of plant metabolites are synthesized at different regions of Endoplasmic Reticulum (ER). Hence, one could also expect the target diterpenes to be attached to the highly developed surface of ER. Additionally, some *Salvia* species contain diterpenes in glandular trichomes that cover the surface of leaves. The IM and ER are characterized by high specific surface area (surface-to-volume ratio). Consequently, on the level of the cell compartments, certain molecules of carnosic acid are adsorbed, i.e., directly attached to the surface, while the others are stored in plastids and trichomes and are not strongly bound up with the plant matrix. The described model of storage mechanisms explains the observed equilibrium data discussed in detail in Sect. 3.

Usually (Bucić-Kojić et al., 2013; del Valle and Urrego, 2012; Perrut et al., 1997) the freely available solute, not attached to membranes in our case, is considered separately from the adsorbed fraction described by the linear adsorption model. This approach does not account for possible cooperative effects, i.e., lateral interactions between adsorbed molecules (Ayawei et al., 2017; Goutelle et al., 2008; Liu, 2015; Stefan and Le Novère, 2013; Wyman and Gill, 1990). The lateral interactions are typical for the adsorption of macromolecules on membranes and proteins (enzymes) containing multiple sorption sites. These systems are non-ideal. Quantitatively, the non-ideal desorption can be described in terms of the so-called Hill (or Hill-Langmuir) adsorption isotherm. It was originally proposed to interpret the sorption of oxygen by haemoglobin and since then was successfully used to fit experimental data from various physicochemical reactions (Goutelle et al., 2008).

The aim of the present study is to investigate the binding of abietane diterpenoids to the plant matrix in *S. officinalis* within the framework of the Hill-Langmuir desorption isotherm and suggest a general optimum protocol to estimate the total content of the target compounds. Three extraction techniques, reflux, Soxhlet, and percolation, are used to constrain the two parameters of the Hill-Langmuir equation as well as the total and freely available content of target metabolites. Corresponding (inverse) problem is highly non-linear, and its solution requires analysis of naturally complex information. Only a maximum-likelihood model (Menke, 2012) alone is not sufficient here, and the resolution power of the data becomes also of primary importance. This implies application of the Monte Carlo method (Menke, 2012) developed by Tarantola and Mosegaard (Cordua et al., 2012; Mosegaard, 1998; Tarantola, 2005). Such an approach also allows estimation of the model parameters uncertainty induced by the measurement errors of different origin.

2. Materials and methods

2.1. Sample preparation and reagents

S. officinalis (L.) was the commercial sample available from ZAO "St-Medifarm" through pharmacies in the form of tea bags. The package description stated that the bags contained dried ground leaves with the characteristic size less than 2 mm determined by the sieve analysis. The material was additionally milled in the laboratory using the laboratory grain mill LGM-1 (OLIS LLC, Russia) to significantly decrease the characteristic size of particles. The average diameter of the final particles was less than 150 μm. About 60 g of ground raw material was prepared in this way. The whole mass was well-mixed each time before the preparation of samples for the extraction. The solid (dry) content of ground leaves was determined as 92%. Hereinafter, the sample mass is given as the dry mass, and the diterpene content is reported in mg g^{-1} of dry plant weight. Analytical balances GR-200 from A&D Company, Japan, with the standard measurement accuracy of 0.1 mg were used to weigh each sample. Petroleum ether (40–70 °C) was of analytical grade from JSC "EKOS-1", Moscow, Russia.

2.2. Extraction at reflux

The dynamics of extraction of phenolic diterpenes by PE at reflux had been studied earlier (Khaliullina et al., 2017; Salamatin et al., 2015). The same experimental conditions were used in the present work. Each sample (~1 g, measured precisely) was mixed with the volume of 50, 100, 200, or 400 mL of PE in the flask at the room temperature. Then, the flask was connected to the reflux system, and heated by boiling water. Typically, after 2–4 min the solvent started to boil.

Once the raw material is mixed with the solvent, the experimental run results in a single data point: equilibrium concentration $c = c^{\infty}$ of diterpenes in the solution after the time T of extraction. Our previous results (Khaliullina et al., 2017) show that ~30 min is typically sufficient to reach the equilibrium distribution of target compounds in the flask. The time was doubled in the present work with T =60 min.

Some samples were subject to double extraction, i.e., the same plant material was extracted one time at a fixed solvent-to-solid ratio L, separated from the solution, and then mixed with the new portion of pure solvent at the same ratio to be extracted again.

Extraction was terminated by removing the flask from the heating element and cooling under a stream of the cold running water. The liquid solution was filtered through the Whatman no. 4 paper filter to separate it from dispersed plant particles.

Experimental conditions (exact sample mass, total solvent volume and corresponding specific volume) are listed in Supplementary Information (SI), Table S1, Sect. 1.1.

2.3. Percolation

In these experimental series, a 1 g-sample of the raw material (measured precisely) was placed on the Whatman no. 4 paper filter that was fixed above the collecting flask, initially empty. Doses of 10–15 mL of pure hot, boiling solvent were sequentially poured on the sample and percolated, led by gravity into the collecting flask below. The contact time between the solid and the solvent was 3–4 min per each 15 mL-portion of the solvent. The concentration of diterpenes in the solution in the flask was determined each time when a new portion of 50 mL of the pure solvent was percolated.

Once 200 mL of solvent had been percolated, the total extracted mass of target compounds was measured, and the depleted sample was subject to extraction at reflux for 60 min, using 100 mL of solvent. Two samples were examined according to this protocol (combination of percolation and extraction at reflux). Results are given in Table S2 of SI Sect. 1.2.

2.4. Soxhlet extraction

Five samples were extracted in the Soxhlet apparatus for 10 h each to determine the lower estimate of the total content of diterpenes in the raw material. The average value for the extracted content of target compounds was 36.4 ± 1.36 mg g^{-1} dry plant weight.

2.5. Determination of extracted mass of target compounds

Quantification of the total diterpenes content was based on spectrophotometric method and Beer-Lambert law (Ingle and Crouch,

1988). A 5 mL aliquot of extract was used for this analysis in LAMBDA 25 spectrophotometer (Perkin Elmer, United States) with the cell thickness $d = 1$ cm. The corresponding analytical wavelength is 285 nm (Bicchi et al., 2000; Carvalho et al., 2005; Thorsen and Hildebrandt, 2003).

This procedure measures the diterpene fraction mainly comprised of carnosic acid and carnosol as equivalent to carnosic acid. The two compounds have close molar masses, 332.44 g mol^{-1} and 330.42 g mol^{-1}, respectively. The absorbance of 1 g of carnosic acid per 1 dL of PE solution in 1 cm cell, i.e. specific absorbance coefficient, is $E^{1\%}_{1cm}$ = 40.92 dL cm^{-1} g^{-1} (Moreno et al., 2006; Zilfikarov and Zhilin, 2007).

If required, solutions were additionally diluted to stay within the applicability region of the Beer-Lambert law (see Sect. 2.6 for details). The correlation between the diterpene concentration c in the liquid solution and the absorbance A is given by the following equation

$$c = An/E^{1\%}_{1cm}d, \quad x = cL \tag{1}$$

where n – dilution factor, x – specific extracted mass of diterpenes per dry unit mass of the solid sample.

2.6. Dilution of aliquot

To determine the applicability region of the Beer-Lambert law, the test solution was prepared in the course of 20-min extraction. The dry sample mass was 0.9462 g, solvent volume – $V = 200$ mL ($L = 211.37$ mL g^{-1}). The aliquots of solution were diluted with the dilution factor n = 2, 4, 5, and 10. For each dilution factor, two aliquots were prepared, and the absorbance of each was measured at the analytical wavelength two or three times. Dilution factors 2, 4, and 5 span the interval of $0.095 < A < 0.3$, and the corresponding calculated value of x = 2.54% remained constant in all tests, indicating applicability of the Beer-Lambert law within the above stated range of A. In contrast, the original non-dilute solution demonstrated the absorbance of 0.52, and Eq. (1) at $n = 1$ yielded the overestimated result x = 2.7%. The underestimated value x = 2.22% was obtained for the dilution factor $n = 10$ at A = 0.043. More details are given in SI, Sect. 1.3.

Thus, the dilution factor n was determined in each experiment by trials and errors to provide the measured absorbance value A to stay between 0.1 and 0.3.

2.7. Inverse Monte Carlo method

Statistical analysis of the collected data was carried out with the use of the inverse Monte Carlo sampling method (Cordua et al., 2012; Menke, 2012; Mosegaard and Sambridge, 2002; Tarantola, 2005). The output of the algorithm is the probabilistic estimates of the model parameters in terms of the probability density as a function of these parameters considered as random variables.

This method is based on *a priori* information about model parameters and modifies it taking into account the *a posteriori* measurement statistics of the data available from various sources and experimental protocols. In our case, *a priori* information, being the knowledge available before the experiments, is the preliminary estimates and ranges of the solution concentration, absorbance, total content, and other characteristics of equilibrium desorption isotherm that are essentially non-negative quantities. Introducing a reasonable upper limit for each quantity, the corresponding random variable is considered to be uniformly distributed on the respective interval. Its exact value is not known *a priori*.

The *a posteriori* information about model parameters is the data obtained in the research. In our case, multiple extractions (Khaliullina et al., 2017) at various specific volumes L (Sect. 3.2), percolation (Sect. 3.3), and Soxhlet extractions (Sect. 2.4) were conducted. The Monte Carlo sampling method is the rigorous way to constrain the intervals introduced as the *a priori* information and decrease the uncertainty of the model parameters. In particular, the results of Soxhlet extraction experiments constrain the lower boundary of interval for the total content of target metabolites.

3. Results and discussion

3.1. Kinetics of extraction process

Extraction kinetics of diterpenes with PE from finely ground material has been previously discussed in Khaliullina et al., 2017 and Salamatin et al., 2015. The results are briefly summarized as follows. The solute concentration in the solvent phase almost instantaneously, that is as soon as the solvent starts to boil, grows up to 70–85% of the equilibrium value, c^{∞}, at the fine grinding of the raw material. The equilibrium distribution is reached within the next 20–30 min. It remains constant up to 120 min of extraction, indicating that the solute degradation does not take place at the boiling temperature of the PE. A similar kinetics is observed in extraction of phenolic compound from the grape seeds, and in other cases (Bucić-Kojić et al., 2013; Egorov et al., 2014; Egorov and Salamatin, 2015).

3.2. Effect of specific volume on equilibrium phase distribution of diterpenes

Analysis of the equilibrium distribution of target diterpenes between solid and liquid phases is carried out for the specific volume range of 50 mL $g^{-1} < L <$ 400 mL g^{-1} following the protocol of Khaliullina et al., 2017. The results are presented in Fig. 2.

First, we note that the 20 min extraction is not sufficient to obtain the equilibrium distribution of the target compounds between solid and liquid phases. This is in accordance with the previously published results (Khaliullina et al., 2017).

Second, it should be emphasized that neither the solvent saturation

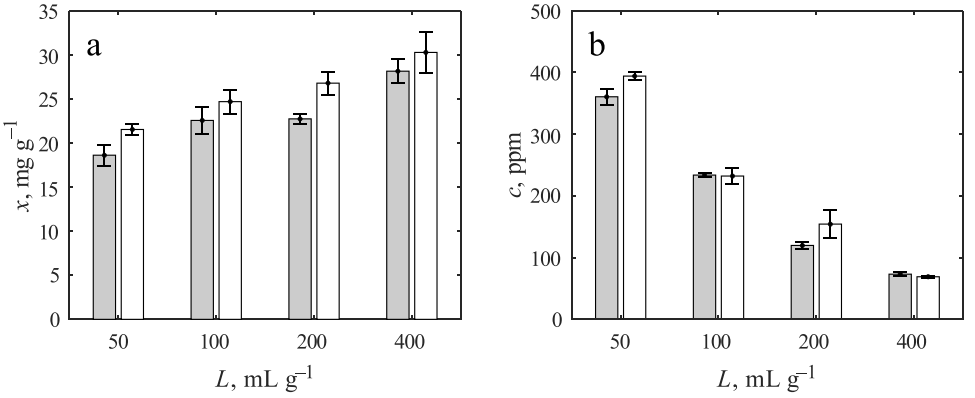

Fig. 2. (a) Specific mass $x = cL$ of extracted solute and (b) solution concentration c at extraction times T = 20 and 60 min (grey and white bars respectively) at reflux versus L-ratios (abscissa), see SI for the exact values of L, Tables S1 and S4. Specific mass x provides a lower estimate of the total content y_0 of diterpenes in the raw material. Error bars are standard deviations based on two measurements.

by diterpenes nor the complete extraction has been achieved within the test range of equilibrium solute concentrations, 70 ppm < c^∞ < 390 ppm. Thus, the observed value of c^∞ steadily decreases with specific volume L, and the value of the extracted specific mass $x = c^\infty L$ is not constant as well. The respective increase in specific mass x is about 50%, from 21.5 mg g^{-1} dry plant weight at L = 50 mL g^{-1} to 30.3 mg g^{-1} dry plant weight at L = 400 mL g^{-1}, while the value of L varies by almost one order of magnitude. This observation proves that the irreversible desorption is the governing mechanism of the extraction. Consequently, single extraction at reflux does not lead to the complete leaching of target compounds. The results of multiple extractions (Khaliullina et al., 2017) discussed in Sect. 3.3 confirm this statement.

3.3. Percolation experiments

Let us compare the efficiency of percolation with the single extractions at reflux at different specific volumes L (see Figs. 2a and 3). Percolation of 50 mL of solvent per 1 g of the solid sample (x = 21 mg g^{-1}) is practically equivalent to the much longer extraction at reflux (x = 21.5 mg g^{-1}) with the same specific volume L = 50 mL g^{-1}. Importantly, sequential filtration of 200 mL g^{-1} of solvent results in the same amount of diterpenes (x = 29.7 mg g^{-1}) as the extraction at reflux (x = 30.3 mg g^{-1}) with the two times higher solvent consumption at L = 400 mL g^{-1}. Finally, when the raw material after percolation was subjected to the extraction at reflux with L = 100 mL g^{-1}, additional amount of x = 7.3 mg g^{-1} (see Fig. 3, bar 5) was obtained, and the total extracted mass made up 36.9 mg g^{-1}, that is about 23% more than the single extraction at reflux delivered at L = 400 mL g^{-1}. Evidently, these observations demonstrate the importance of desorption model development and wide possibilities of optimizing the desorption process to achieve the efficient use of labour, time, and materials.

The experimental results discussed above are interpreted in Sect. 3.4 in terms of the mass balance of target compounds in the system of the raw material and the solvent in the framework of corresponding model of the equilibrium desorption isotherm. In Sect. 3.5, the total content y_0 of abietanes (carnosic acid and its derivatives) in the raw material is estimated, and significantly non-linear behavior, i.e., deviation from Henry's law, of the isotherm is demonstrated. The diverse data on the extractability of solute subject to various uncertainties is analysed using the inverse Monte Carlo sampling approach (Cordua et al., 2012; Menke, 2012; Tarantola, 2005).

3.4. Equilibrium phase distribution of diterpenes

It is assumed that only extraction at reflux conditions correspond to the equilibrium distribution of target compounds determined by the Hill-Langmuir desorption isotherm. Percolation experiment is not sufficiently long to attain the equilibrium (c^∞, y^∞) point, and the temperature in the thimble of the Soxhlet apparatus is lower than the one in the flask at reflux. Nevertheless, followed by extraction at reflux, all other preliminary treatments of the raw material samples can be taken into account in the mass balance as the pre-extracted amount Y_0 of the target compounds.

With this in mind, first, let us consider the extraction at reflux when the plant material is added to the pure solvent. Metabolites diffuse with time to the liquid phase; simultaneously, the concentration increases, $c \to c^\infty$, and the content in the plant matrix decreases, $y \to y^\infty$, until the equilibrium distribution is reached after a sufficiently large time. Various equilibria can be sampled performing percolation followed by the extraction at reflux. The total content of metabolites decreases by a measured value Y_0 after percolation as demonstrated, for example, by the bar 4 in Fig. 3. The final product x is given by the bar 6 as the sum of the results of all consecutive treatments of the sample, bars 4 and 5. Alternatively, different solvent-to-solid ratios can be used or multiple extractions at reflux can be performed. In the latter case, $Y_0 = 0$ for the first extraction, and, for the second run, Y_0 is equal to $x = c^\infty L$ obtained at the first run and etc.

The particle size is sufficiently small to assume uniform distribution of y in the solid phase. The same we assume for the liquid phase introducing an average concentration $c = c(t)$ of abietane diterpenoids in the solution. Thus, the solution concentration c, current diterpene content y, and initial content y_0 are related through the mass balance equation

$$y(t) = (y_0 - Y_0) - c(t)L, \quad x = cL \tag{2}$$

$$c|_{t=0} = 0, \quad y|_{t=0} = y_0 - Y_0, \quad c|_{t=\infty} = c^\infty, \quad y|_{t=\infty} = y^\infty$$

The desorption isotherm predicts the ultimate, equilibrium distribution (c^∞, y^∞) that is attained at infinite extraction time. Particular isotherm (Ayawei et al., 2017; del Valle and Urrego, 2012; Liu, 2015; Perrut et al., 1997) reflects our understanding of the storage mechanisms and the nature of bonds that bind the target compounds to the plant matrix. The so-called cooperative adsorption (or binding) (Liu, 2015) occurs, when the (lateral) interactions between molecules on the active surface play a significant role. As discussed in the introduction, at least two fractions of target compounds characterized by different storage mechanisms can be distinguished in our case. One is assumed to be strongly bound to the plant matrix, mainly the endoplasmic reticulum and intracellular membranes, and the other is freely available for extraction in chloroplasts. Accordingly, the respective contents are designated hereinafter as y_h and y_e, and the total content $y_0 = y_e + y_h$.

Let us first consider single extraction at reflux with $Y_0 = 0$. It is assumed that the freely available molecules diffuse with a much higher rate. They dissolve in the solvent and almost instantaneously increase the current solution concentration c, as discussed in Sect. 3.1. Then, desorption of strongly bound molecules takes place at much lower rate and is interpreted in the framework of the Hill correlation (Stefan and Le Novère, 2013)

$$y^\infty = \frac{y_h}{1 + (c_0/c^\infty)^k} \tag{3}$$

Here, the Hill index k describes the cooperativity of target compounds binding. The cooperativity is positive at $k > 1$ if binding of a target compound molecule (ligand) increases the receptor's (membrane's) apparent affinity, and hence increases the chance of another ligand molecule binding. The cooperativity is called negative if opposite behavior is observed at $0 < k < 1$. The parameter $K_d = c_0^k$ is the apparent dissociation constant of sorption/desorption reactions. The scaling factor c_0 is the concentration that produces half occupation, $y^\infty = y_h/2$ at $c^\infty = c_0$.

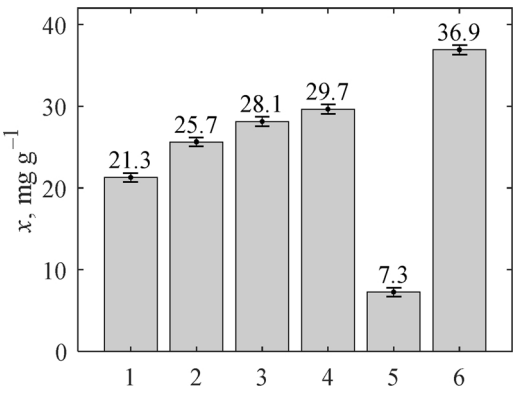

Fig. 3. Results of percolation. Bars 1–4: accumulated x-value obtained after filtration of every 50 mL of solvent; Bar 5: extraction of the same, depleted plant material with residual diterpenes at reflux for 60 min at L = 100 mL g^{-1}; Bar 6: total extracted amount of diterpene acids within the experiment (the sum of bars 4 and 5).

The system of the two equations, Eqs. (2) and (3), can be solved for the (c^∞, y^∞)-distribution of target compounds between phases at equilibrium for any given L, total content y_0, and parameters of the isotherm. Substitution of y^∞ given by Eq. (3) into the mass balance Eq. (2) yields

$$\frac{y_h}{1+(c_0/c^\infty)^k} = (y_e + y_h - Y_0) - c^\infty L, \quad y_0 = y_e + y_h \tag{4}$$

This non-linear relationship implicitly determines the equilibrium solute concentration c^∞, deduced in the experimental runs from Eq. (1), as the function of model parameters y_e, y_h, k, c_0 at given L and Y_0.

3.5. Monte Carlo sampling approach

Based on the available data, model (4) can be constrained and its parameters can be inferred through the solution of the so-called inverse problem, using the Monte Carlo sampling method (Cordua et al., 2012; Menke, 2012; Mosegaard, 1998; Tarantola, 2005). The best-fit values of the model parameters minimize the so-called misfit function $S(y_e, y_h, n, c_0)$. It is the measure of distance between the observed data (superscript *exp*) and the theoretically predicted values of the equilibrium solution concentration c^∞ at given specific volume L and pre-extracted value Y_0

$$S(y_0, y_h, n, c_0) = \sum_i \frac{|\tilde{c}_i^{exp} - \tilde{c}^\infty(L_i, Y_{0,i}|\tilde{y}_e, \tilde{y}_h, \tilde{n}, \tilde{c}_0)|}{\sigma_c}$$

$$\tilde{c}_i^{exp} = \ln c_i^{exp}, \quad \tilde{c}^\infty = \ln c^\infty, \quad \tilde{y}_e = \ln y_e, \quad \tilde{y}_h = \ln y_h, \quad \tilde{n} = \ln n, \quad \tilde{c}_0 = \ln c_0$$

Here, index i spans over all experimental runs (except for Soxhlet extraction) represented by the observed triplets $(\tilde{c}_i^{exp}, Y_{0,i}, L_i)$. The log-Laplace distribution of random errors is employed for the observed solute concentration c to construct the misfit function in our study. Log-type distributions are typical for non-negative quantities, while the Laplace distribution, as an absolute norm with the exponent factor equal to unity, assigns commensurable weights to each data point (Menke, 2012) and remains stable with respect to small number of outliers in contrast to (log-) normal distributions (Tarantola, 2005) with the exponent factor equal to two.

Each parameter is considered as a random variable, and their joint probability distribution function $f(y_e, y_h, n, c_0)$ is proportional to the likelihood function $\ell = \exp(-S)$, where σ_c is understood as the variance of the distribution. There are multiple sources of random errors that arise on the stages of sample and solvent preparation, separation of liquid solution from dispersed solid phase, making of aliquot, dilution, measurement of absorbance etc. The combined uncertainty σ_c is estimated based on the extraction data at $L = 100$ mL g^{-1} as the average absolute deviation from the median of the sample. Eight data points are available, and the assumed estimate is $\sigma_c = 0.0572$.

As *a priori* information, two constraints, 40 mg g^{-1} $< y_0 <$ 70 mg g^{-1}, were introduced. The lower estimate is based on the results of double extraction at reflux at $L = 400$ mL g^{-1}. The upper bound is chosen to be slightly higher than the estimate available from literature (Jassbi et al., 2013).

The obtained results of the Monte-Carlo resolution analysis are discussed below.

3.6. Discussion

3.6.1. Best-fit parameters of desorption isotherm

First, let us discuss the deduced best-fit model parameters. They are $y_0 = 59$ mg g^{-1}, $y_e = 20$ mg g^{-1}, $y_h = 39$ mg g^{-1}, $c_0 = 43.4$ ppm, and $k = 1.21$. The corresponding dependence of interphase equilibrium distribution of abietanes on L is presented in Fig. 4. According to the mass balance, Eq. (2), the system evolution during the single extraction at reflux from the starting moment of mixing in the flask towards the equilibrium can be represented as a straight line on the (c, y) plane with time $0 < t < \infty$ considered as a parameter along the trajectory. Its initial point and slope are determined by $y_0 - Y_0$ and L, respectively, while the equilibrium distribution of the target compounds (c^∞, y^∞) is the end-point of the trajectory that falls, by definition, on the desorption isotherm (smooth solid curve in Fig. 4a).

Each calculated trajectory in Fig. 4a corresponds to the best-fit values and starts from the same point, $c = 0$, $y = y_0 = 59$ mg g^{-1}. Dashed broken line illustrates the trajectory of two sequential extractions (at $L = 400$ mL g^{-1}) of the same sample of the raw material. The horizontal segment reflects the separation of the dispersed phase from the solution, and mixing with the new portion (400 mL g^{-1}) of the pure solvent. The total content for the second extraction has to be reduced by the amount $Y_0 = 33.1$ mg g^{-1} (theoretical value) extracted at the first step, and the initial point for the last segment is $y_0 - Y_0 = 25.9$ mg g^{-1}.

The shape of the equilibrium desorption isotherm in Fig. 4a demonstrates the asymptotic saturation at the level of $y = y_h$ and explains the necessity and efficiency of percolation or multiple extractions to proceed with further depletion of the raw material. In other words, at the beginning of extraction the freely available content of the target compounds, $y_e = y_0 - y_h$, is separated first. The solution concentration almost instantaneously grows up to $c \approx y_e/L < c^\infty$ following the corresponding (c, y)-trajectory towards the desorption isotherm, while the content of target components in the plant matrix drops down to $y \approx y_h < y_0$ (see the dash-dotted line in Fig. 4a). Then, a further increase of concentration is observed along the trajectory. Depending on L, the increase is relatively small with $y^\infty \approx y_h$ at $L < 100$ mL g^{-1}, but significant at $L > 200$ mL g^{-1}, resulting in $y^\infty < y_h$ (consider the set of straight lines in Fig. 4a). Obviously, the solvent "strength" non-linearly increases with the decrease in the solute concentration, getting

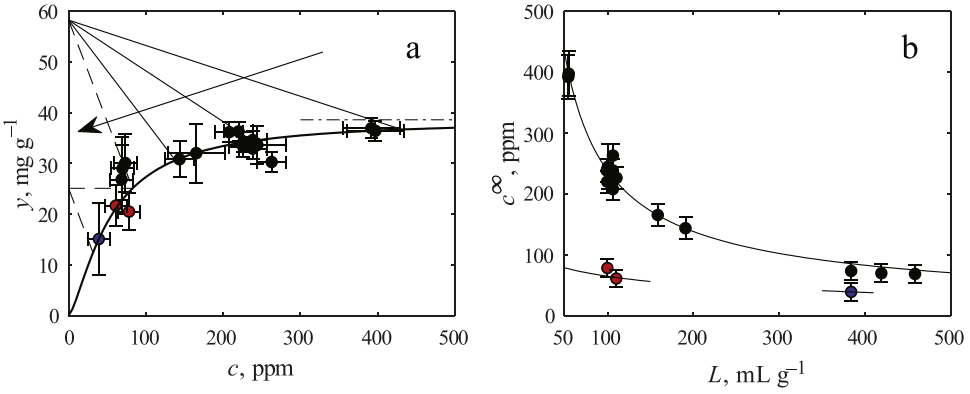

Fig. 4. The equilibrium extraction data (points with error bars) and (a) the best-fit equilibrium desorption isotherm, y^∞ versus c^∞, and (b) the equilibrium solution concentrations c^∞ versus the specific volume L. Markers: the black colour – first extraction at reflux ($Y_0 = 0$ in the mass balance), the red colour – extraction after percolation ($Y_0 = 2.98\%$), and the blue colour – second extraction at reflux at $L = 400$ mL g^{-1} ($Y_0 = 2.81\%$). The black thin segments in (a) are the calculated mass balance trajectories, Eq. (2), corresponding to the best-fit model parameters, Eq. (3), at $L = \{50, 100, 200, 400\}$ mL g^{-1}. The arrow indicates the direction of L increase. The dashed broken line with horizontal segment is the trajectory of the double extraction at the same $L = 400$ mL g^{-1}. The horizontal dash-dotted segment is the asymptotic value of the isotherm equal to y_h.

sufficiently large to “tear the adsorbed molecules off” the membranes.

The observed equilibrium solute concentration c^{∞} is plotted versus corresponding specific volume L in Fig. 4b. A set of curves is obtained for different pre-treatment parameters Y_0. The main curve that spans over the entire range of L corresponds to $Y_0 = 0$. The black circles show the data corresponding to single extractions. Two other curves correspond to non-zero Y_0 conditions and calculated for a smaller L-interval. Two red points at $L = 100$ mL g^{-1} are obtained after percolation experiment with the extracted amount of diterpenes $Y_0 = 29.8$ mg g^{-1}. The blue point is the second extraction at 400 mL g^{-1} in the series of two experiments with the same sample.

3.6.2. Resolution analysis

While the best-fit values always exist, in general, it does not mean that they are resolved sufficiently well by the observed data, and the corresponding variances are reasonably small. Here, the resolution analysis is performed by means of the random-walk sampling (Mosegaard, 1998; Tarantola, 2005), and the obtained histograms of the marginal probability densities are shown in Fig. 5.

The calculated means and standard deviations for y_e, y_h, y_0, k, and c_0 are respectively 18.7 ± 2.9 mg g^{-1}, 40.4 ± 8.3 mg g^{-1}, 59.1 ± 7 mg g^{-1}, 1.422 ± 0.457, and 55.8 ± 16 ppm. Observe the slight deviation of the mean from the best-fit values, i.e. modal ones. It is due to unsymmetrical marginal distributions with heavy tails. The standard deviations are within 30% of the mean values, and from Fig. 5d one can observe that the cooperative adsorption is more likely to be positive with $k \geq 1$.

Although being asymmetric, the histograms for y_e, k, and c_0 in Fig. 5a, d, and e are rather sharp, and the latter model parameters are thought to be relatively well resolved. At the same time, practically uniform sampling frequency is observed in Fig. 5c for $y_0 > 50$ mg g^{-1} up to the imposed *a priori* bound $y_0 = 70$ mg g^{-1}. Additional numerical experiments (not discussed here) show that this constant-probability-density zone extends to even higher values of the total content y_0 with

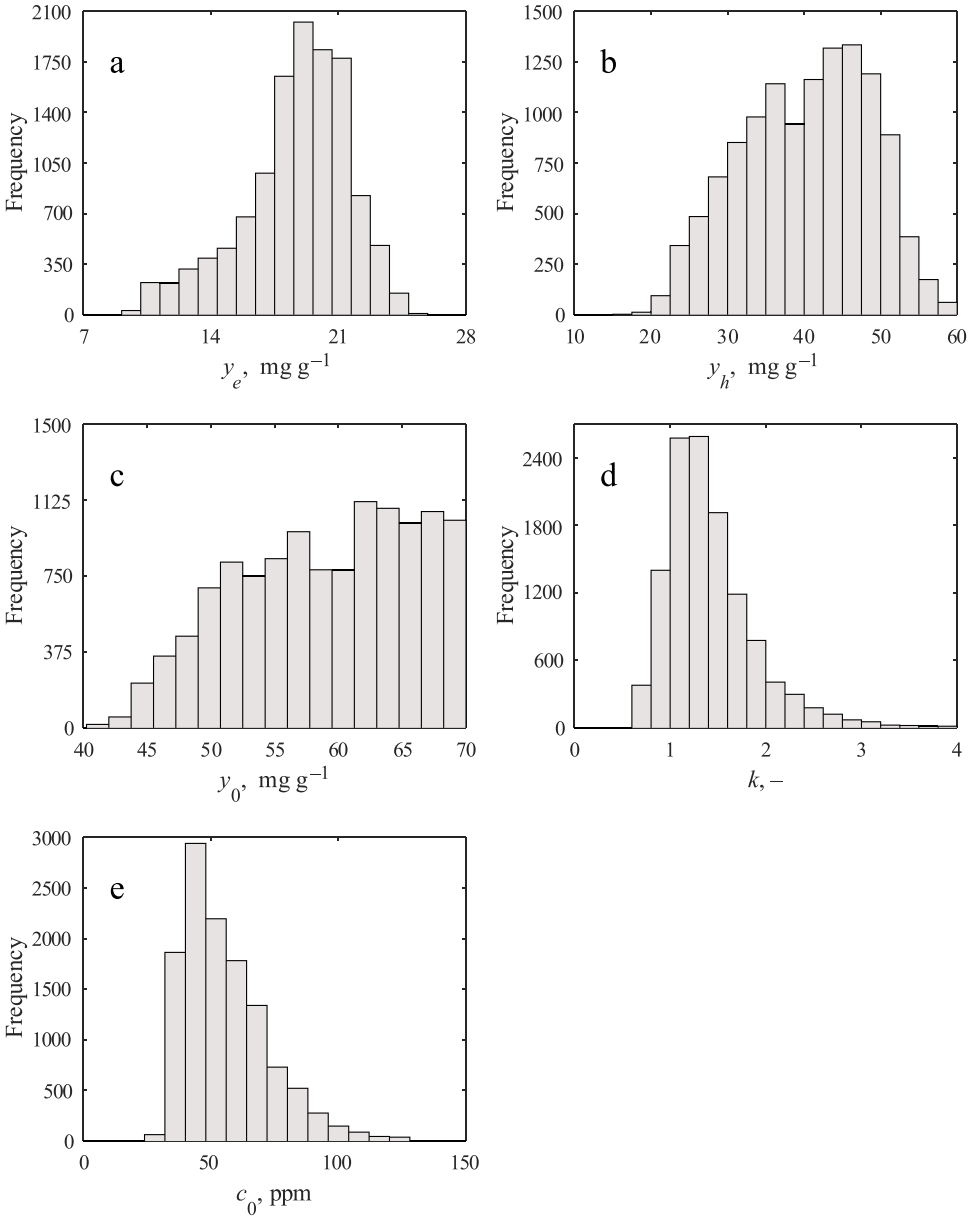

Fig. 5. Histograms of marginal probability densities of equilibrium isotherm parameters of Hill equation, (a) target compounds content freely available for extraction y_e, (b) target compounds content bound to the plant matrix y_h, (c) total content of target compounds y_0, (d) the Hill coefficient (index) k, and (e) concentration scaling factor for the equilibrium desorption isotherm c_0.

increase of its upper bound. Accordingly, the histogram of y_h-probability distribution in Fig. 5b also becomes broader. Thus, regular laboratory-scale experiments, such as multiple extractions at reflux, percolation, and Soxhlet extraction considered in our study, do not allow for the reasonable estimation of the upper limit of the target content y_h, bound to the plant matrix, as well as the total content y_0. Special experiments are needed for the better resolution of these characteristics. Yet, the lower estimate, $y_0 > 50–55\ \mathrm{mg\,g^{-1}}$, seems to be well established and is in agreement with the published data (Jassbi et al., 2013).

4. Conclusion

The PE is tested as a solvent for extraction of diterpene acids and their derivatives from *S. officinalis* (L.). The non-polar solvent dissolves the lipophilic compounds, however, the sorption effects hinder the extraction kinetics, and the complete extraction with a single portion of the solvent is not possible. The observed binding of target metabolites to the plant matrix is positively cooperated. A simple, linear Henry's desorption isotherm cannot capture these effects. Thus, the particular system of *S. officinalis* and PE differs from many other pairs of plant matrices and solvents.

It is demonstrated that percolation is evidently more efficient than extraction at reflux both in time, consumed materials, and the level of the raw material depletion. The key factor here is the distribution of the available solvent by smaller portions among the sequential extraction steps. Once the freely available solute is depleted, the larger contact times are required to reach an equilibrium, and extraction at reflux could follow the percolation to increase the extraction efficiency.

As for the deduced estimates of the model parameters of the non-linear desorption isotherm, the freely available fraction of the target compounds, which requires minimum consumption of solvent, is found to be $20.0 \pm 2.9\ \mathrm{mg\ g^{-1}}$ dry raw material. Another principal characteristic (a measure of the extraction protocol efficiency) is the total content of the target compounds. Our experimental runs of the double extraction at reflux, predict that this quantity is not less than $43.1 \pm 5.2\ \mathrm{mg\ g^{-1}}$ of dry raw material. The Monte Carlo resolution analysis based on all our laboratory data suggests a lower estimate of $50–55\ \mathrm{mg\,g^{-1}}$ of dry raw material, which is in agreement with an independent study (Jassbi et al., 2013). However, the upper bound of the total content cannot be reliably deduced from the standard laboratory experiments, and $60–70\ \mathrm{mg\,g^{-1}}$ dry plant weight seems to be a reasonable estimate of the target compounds mass that can be separated from the plant matrix in practice.

Declaration of Competing Interest

None.

Acknowledgements

This work was supported by the Russian Foundation for Basic Research and the Academy of Science of Republic of Tatarstan through the grant no. 18-41-160001 and 19-31-60013. The funding due to the Russian Government Program of Competitive Growth of Kazan Federal University is also acknowledged. We are grateful to I. F. Safin of the Department of Criminal Process and Criminalistics (Kazan Federal University) for providing the access to lab microscopes. We are thankful to Dr. H. Sovova for her kind advises regarding the most relevant literature, and to anonymous referees for their constructive comments.

Appendix A. Supplementary data

Supplementary material related to this article can be found, in the online version, at doi:https://doi.org/10.1016/j.indcrop.2019.111909.

References

Anastasaki, E., Zoumpopoulou, G., Astraka, K., Kampoli, E., Skoumpi, G., Papadimitriou, K., Tsakalidou, E., Polissiou, M., 2017. Phytochemical analysis and evaluation of the antioxidant and antimicrobial properties of selected herbs cultivated in Greece. Ind. Crops Prod. 108, 616–628. https://doi.org/10.1016/J.INDCROP.2017.06.066.

Ayawei, N., Ebelegi, A.N., Wankasi, D., 2017. Modelling and interpretation of adsorption isotherms. J. Chem.-NY. 2017, 1–11. https://doi.org/10.1155/2017/3039817.

Bicchi, C., Binello, A., Rubiolo, P., 2000. Determination of phenolic diterpene antioxidants in rosemary (Rosmarinus officinalis L.) with different methods of extraction and analysis. Phytochem. Anal. 11, 236–242. https://doi.org/10.1002/1099-1565(200007/08)11:4<236::AID-PCA503>3.0.CO;2-B.

Birtić, S., Dussort, P., Pierre, F.-X., Bily, A.C., Roller, M., 2015. Carnosic acid. Phytochemistry 115, 9–19. https://doi.org/10.1016/J.PHYTOCHEM.2014.12.026.

Bucić-Kojić, A., Sovová, H., Planinić, M., Tomas, S., 2013. Temperature-dependent kinetics of grape seed phenolic compounds extraction: experiment and model. Food Chem. 136, 1136–1140. https://doi.org/10.1016/J.FOODCHEM.2012.09.087.

Carvalho, R.N., Moura, L.S., Rosa, P.T.V., Meireles, M.A.A., 2005. Supercritical fluid extraction from rosemary (Rosmarinus officinalis): kinetic data, extract's global yield, composition, and antioxidant activity. J. Supercrit. Fluids 35, 197–204. https://doi.org/10.1016/J.SUPFLU.2005.01.009.

Chang, S.S., Ostric-Matijasevic, B., Hsieh, O.A.L., Huang, C.-L., 1977. Natural antioxidants from Rosemary and Sage. J. Food Sci. 42, 1102–1106. https://doi.org/10.1111/j.1365-2621.1977.tb12676.x.

Cordua, K.S., Hansen, T.M., Mosegaard, K., 2012. Monte Carlo full-waveform inversion of crosshole GPR data using multiple-point geostatistical a priori information. Geophysics 77, H19–H31. https://doi.org/10.1190/geo2011-0170.1.

del Valle, J.M., Urrego, F.A., 2012. Free solute content and solute-matrix interactions affect apparent solubility and apparent solute content in supercritical CO_2 extractions. A hypothesis paper. J. Supercrit. Fluids 66, 157–175. https://doi.org/10.1016/J.SUPFLU.2011.10.006.

Durling, N.E., Catchpole, O.J., Grey, J.B., Webby, R.F., Mitchell, K.A., Foo, L.Y., Perry, N.B., 2007. Extraction of phenolics and essential oil from dried sage (Salvia officinalis) using ethanol–water mixtures. Food Chem. 101, 1417–1424. https://doi.org/10.1016/J.FOODCHEM.2006.03.050.

Egorov, A.G., Salamatin, A.A., 2015. Bidisperse shrinking core model for supercritical fluid extraction. Chem. Eng. Technol. 38. https://doi.org/10.1002/ceat.201400627.

Egorov, A.G., Salamatin, A.A., Maksudov, R.N., 2014. Forward and inverse problems of supercritical extraction of oil from polydisperse packed bed of ground plant material. Theor. Found. Chem. Eng. 48. https://doi.org/10.1134/S0040579514010011.

Goutelle, S., Maurin, M., Rougier, F., Barbaut, X., Bourguignon, L., Ducher, M., Maire, P., 2008. The Hill equation: a review of its capabilities in pharmacological modelling. Fund. Clin. Pharmacol. 22, 633–648. https://doi.org/10.1111/j.1472-8206.2008.00633.x.

Huang, S.-W., Frankel, E.N., Schwarz, K., Aeschbach, R., German, J.B., 1996. Antioxidant activity of carnosic acid and methyl carnosate in bulk oils and oil-in-water emulsions. J. Agric. Food Chem. 44, 2951–2956. https://doi.org/10.1021/JF960068R.

Ibrahim, T.A., 2012. Chemical composition and biological activity of extracts from Salvia bicolor Desf. Growing in Egypt. Molecules 17, 11315–11334. https://doi.org/10.3390/molecules171011315.

Ingle, J.D., Crouch, S.R., 1988. Spectrochemical Analysis, 1st ed. Prentice Hall, Englewood Cliffs, New Jersey.

Jassbi, A.R., Miri, R., Alizadeh, M., Asadollahi, M., Massrorbabanari, M., Baldwin, I.T., 2013. Quantification of phenolic diterpenoids and rosmarinic acid in Salvia eremophila and Salvia santolinifolia by LC-DAD-MS. Austin Chromatogr. 1, 1–5.

Khaliullina, A.S., Khaziev, R.S., Salamatin, A.A., 2017. Quantitative determination of diterpene acids in garden sage leaves. J. Anal. Chem. 72. https://doi.org/10.1134/S1061934817070073.

Kintzios, S.E., 2000. Sage: the Genus Salvia. Harwood Academic Publishers.

Kleinig, H., 1989. The role of plastids in isoprenoid biosynthesis. Annu. Rev. Plant Physiol. Plant Mol. Biol. 40, 39–59. https://doi.org/10.1146/annurev.pp.40.060189.000351.

Knudsen, C., Gallage, N.J., Hansen, C.C., Møller, B.L., Laursen, T., 2018. Dynamic metabolic solutions to the sessile life style of plants. Nat. Prod. Rep. 35, 1140–1155. https://doi.org/10.1039/C8NP00037A.

Kolac, U.K., Ustuner, M.C., Tekin, N., Ustuner, D., Colak, E., Entok, E., 2017. The anti-inflammatory and antioxidant effects of *Salvia officinalis* on lipopolysaccharide-induced inflammation in rats. J. Med. Food 20, 1193–1200. https://doi.org/10.1089/jmf.2017.0035.

Kontogianni, V.G., Tomic, G., Nikolic, I., Nerantzaki, A.A., Sayyad, N., Stosic-Grujicic, S., Stojanovic, I., Gerothanassis, I.P., Tzakos, A.G., 2013. Phytochemical profile of Rosmarinus officinalis and Salvia officinalis extracts and correlation to their antioxidant and anti-proliferative activity. Food Chem. 136, 120–129. https://doi.org/10.1016/J.FOODCHEM.2012.07.091.

Liu, S., 2015. Cooperative adsorption on solid surfaces. J. Colloid Interface Sci. 450, 224–238. https://doi.org/10.1016/j.jcis.2015.03.013.

Longaray Delamare, A.P., Moschen-Pistorello, I.T., Artico, L., Atti-Serafini, L., Echeverrigaray, S., 2007. Antibacterial activity of the essential oils of Salvia officinalis L. and Salvia triloba L. cultivated in South Brazil. Food Chem. 100, 603–608. https://doi.org/10.1016/J.FOODCHEM.2005.09.078.

Lu, Y., Yeap Foo, L., 2002. Polyphenolics of Salvia—a review. Phytochemistry 59, 117–140. https://doi.org/10.1016/S0031-9422(01)00415-0.

McGarvey, D.J., Croteau, R., 1995. Terpenoid metabolism. Plant Cell 7, 1015–1026. https://doi.org/10.1105/tpc.7.7.1015.

Menke, W., 2012. Geophysical Data Analysis: Discrete Inverse Theory. Elsevier/Academic

Press.
Miura, K., Kikuzaki, H., Nakatani, N., 2002. Antioxidant activity of chemical components from sage (*Salvia officinalis L.*) and thyme (*Thymus vulgaris L.*) measured by the oil stability index method. J. Agric. Food Chem. 50, 1845–1851. https://doi.org/10.1021/JF011314O.
Moreno, S., Scheyer, T., Romano, C.S., Vojnov, A.A., 2006. Antioxidant and antimicrobial activities of rosemary extracts linked to their polyphenol composition. Free Radic. Res. Commun. 40, 223–231. https://doi.org/10.1080/10715760500473834.
Mosegaard, K., 1998. Resolution analysis of general inverse problems through inverse Monte Carlo sampling. Inverse Probl. 14, 405–426. https://doi.org/10.1088/0266-5611/14/3/004.
Mosegaard, K., Sambridge, M., 2002. Monte Carlo analysis of inverse problems. Inverse Probl. 18, R29–R54. https://doi.org/10.1088/0266-5611/18/3/201.
Munné-Bosch, S., Alegre, L., 2001. Subcellular compartmentation of the diterpene carnosic acid and its derivatives in the leaves of rosemary. Plant Physiol. 125, 1094–1102. https://doi.org/10.1104/PP.125.2.1094.
Okamura, N., Fujimoto, Y., Kuwabara, S., Yagi, A., 1994. High-performance liquid chromatographic determination of carnosic acid and carnosol in Rosmarinus officinalis and Salvia officinalis. J. Chromatogr. A 679, 381–386. https://doi.org/10.1016/0021-9673(94)80582-2.
Perrut, M., Clavier, J.Y., Poletto, M., Reverchon, E., 1997. Mathematical modeling of sunflower seed extraction by supercritical CO_2. Ind. Eng. Chem. Res. 36, 430–435. https://doi.org/10.1021/IE960354S.
Perry, N.B., Anderson, R.E., Brennan, N.J., Douglas, M.H., Heaney, A.J., McGimpsey, J.A., Smallfield, B.M., 1999. Essential oils from dalmatian sage (Salvia officinalis L.): variations among individuals, plant parts, seasons, and sites. J. Agric. Food Chem. 47, 2048–2054. https://doi.org/10.1021/JF981170M.
Raut, J.S., Karuppayil, S.M., 2014. A status review on the medicinal properties of essential oils. Ind. Crops Prod. 62, 250–264. https://doi.org/10.1016/J.INDCROP.2014.05.055.
Salamatin, A.A., Khaziev, R.S., Makarova, A.S., Ivanova, S.A., 2015. Kinetics of bioactive compounds extraction from plant material using boiling solvent. Theor. Found. Chem. Eng. 49, 200–206. https://doi.org/10.1134/S0040579515020116.
Schwarz, K., Ternes, W., 1992. Antioxidative constituents of Rosmarinus officinalis and Salvia officinalis. Z. Lebensm. Unters. Forsch. 195, 99–103. https://doi.org/10.1007/BF01201766.
Stefan, M.I., Le Novère, N., 2013. Cooperative binding. PLoS Comput. Biol. 9, e1003106. https://doi.org/10.1371/journal.pcbi.1003106.
Tarantola, A., 2005. Inverse Problem Theory and Methods for Model Parameter Estimation. Society for Industrial and Applied Mathematics. https://doi.org/10.1137/1.9780898717921.
Thorsen, M.A., Hildebrandt, K.S., 2003. Quantitative determination of phenolic diterpenes in rosemary extracts: aspects of accurate quantification. J. Chromatogr. A 995, 119–125. https://doi.org/10.1016/S0021-9673(03)00487-4.
Wyman, J., Gill, S.J., 1990. Binding and Linkage: Functional Chemistry of Biological Macromolecules. University Science Books.
Xie, Z.-S., Zhong, L.-J., Wan, X.-M., Li, M.-N., Yang, H., Li, P., Xu, X.-J., 2016. Petroleum ether sub-fraction of rosemary extract improves hyperlipidemia and insulin resistance by inhibiting SREBPs. Chin. J. Nat. Med. 14, 746–756. https://doi.org/10.1016/S1875-5364(16)30089-9.
Zilfikarov, I.N., Zhilin, A.V., 2007. Determination of diterpenic acids in the raw materials and preparations of garden sage (Salvia officinalis). Pharmacy 7–9.